Journal of Thermal Analysis and Calorimetry, Vol. 94 (2008) 1, 203–208

THERMAL STABILITY OF SYNTHETIC AURICHALCITE IMPLICATIONS FOR MAKING MIXED METAL OXIDES FOR USE AS CATALYSTS

R. L. Frost, A. J. Locke, M. C. Hales and W. N. Martens*

Inorganic Materials Research Program, School of Physical and Chemical Sciences, Queensland University of Technology
GPO Box 2434, Brisbane Queensland 4001, Australia

TG combined with MS has been used to study the thermal decomposition of a synthetic aurichalcite with varying copper–zinc ratios from 0.1:0.9 to 0.5:0.5. In general, five decomposition steps are observed at 235, 280, 394, 428 and 805°C. The principal mass loss step increases in temperature from 255°C (0.1/0.9) to 300°C (0.5/0.5). MS using ion current curves show that the OH units and carbonate units decompose simultaneously and the two decomposition steps after the main decomposition are attributed to the decomposition of $ZnCO_3$ and $CuCO_3$. A higher temperature decomposition at around 805°C, based upon the ion current curves is assigned to the decomposition of CuO to Cu. The thermal decomposition of aurichalcite offers a method of preparing metal oxides mixed at the molecular level making the thermally activated aurichalcites as suitable for use as catalysts.

Keywords: *aurichalcite, catalysts, decarbonation, dehydration, dehydroxylation, mixed metal oxides, thermogravimetric analysis*

Introduction

The mineral aurichalcite $(Zn,Cu^{2+})_5(CO_3)_2(OH)_6$ is one of a large number of highly coloured copper bearing minerals [1–3]. Aurichalcite forms in the oxidation zones of zinc–copper deposits. Crystals are grass green to pale blue-green [4], acicular and fibrous and often found in aggregates. Aurichalcite will often partially cover red limonite and be associated with such colourful minerals as rosasite, azurite, smithsonite and malachite. Aurichalcite may be confused with rosasite minerals $(Cu^{2+},Zn)_2(CO_3)_2(OH)_2$ because of their similar appearance [5–8]. Rosasite minerals including glaukosphaerite; kolwezite; mcguinnessite are usually more massive and not lamellar [5]. Other related hydroxy carbonates are nullaginite and pokrovskite. It appears that aurichalcite is similar to hydrozincite and both minerals are formed under the same conditions when copper is present in the solution [9]. Williams further states that up to one quarter of the cation sites are occupied by Cu^{2+} [9]. In this work synthetic aurichalcite are prepared with wide variation in the Cu/Zn ratio. Greater concentrations of copper normally give rise to other discrete phases such as malachite and rosasite. Interestingly the range of substitution of other transition metal ions in the hydrozincite lattice is very limited. The minerals in the hydroxy carbonate group have been synthesised because of their potential as catalysts [2]. Further studies of synthetic hydroxy carbonates incorporated Al^{3+} into the structures [10].

Anthony *et al*. reports aurichalcite to be acicular to lathlike crystals with prominent crystal growth along the [010] axis, commonly striated parallel to [001] axis . The mineral is of point group 2/m and space group $P2_1/m$ [11]. Based on the structure the symmetry of the carbonate anion is C_s. The accurate X-ray crystallography of aurichalcite is difficult to obtain because of its very small interwoven needles which makes obtaining single crystal studies difficult [3, 11–13]. Harding *et al*. [13] showed the positions in the structure of aurichalcite are octahedrally coordinated. The atom positions occupied by zinc have tetrahedral coordination.

Recently thermogravimetric analysis has been applied to some complex mineral systems [14–27] and it is considered that TG-MS analysis may also be applicable to many carbonate minerals [18, 28–32]. Very few thermo-analytical and spectroscopic studies of the hydroxy carbonates have been forthcoming and what studies that are available are not new [15, 20, 21, 25–27, 33–42]. To the best of the authors' knowledge no thermo-analytical studies of aurichalcite have been undertaken, especially in recent times [43, 44]; although differential thermal analysis of some related minerals has been published [3].

The thermal decomposition of aurichalcite results in the formation of a mixture of metal oxides of CuO and ZnO. Both these oxides may function as catalysts and photo-catalysts [45–51]. The thermal activation of aurichalcite results in the formation of the oxide mixture, mixed at the molecular level and not at the particle level. In this work we report the thermogravimetric analysis of synthetic aurichalcite with variation in the Cu:Zn ratio.

* Author for correspondence: r.frost@qut.edu.au

1388–6150/$20.00

Akadémiai Kiadó, Budapest, Hungary
Springer, Dordrecht, The Netherlands

Experimental

Synthesis of aurichalcite

The mineral $(Zn,Cu^{2+})_5(CO_3)_2(OH)_6$ was synthesised with different ratios of Cu to Zn. Williams inferred from studies of natural aurichalcite minerals that the highest ratio of Cu to Zn in aurichalcite is 1:3 [9]. A common formula for natural aurichalcite is $Cu_{1.25}Zn_{3.75}(CO_3)_2(OH)_6$. In this work aurichalcites were synthesised with a Cu/Zn ratio of 0.1:0.9, 0.25:0.75, 0.4:0.6 and 0.5:0.5.

Synthesis of ideal products was modelled on the procedure by Fujita *et al*. [52]. A solution of metal ions (M^{2+}) was prepared by mixing appropriate concentrations of 1.5 M $Cu(NO_3)_2$ and $Zn(NO_3)_2$ that correspond to the required metal concentrations. Synthesis of the lower copper concentrations of aurichalcite (Cu<50%) was carried out by adding dropwise 100 mL of a 1.5 M M^{2+} solution via a peristaltic pump to 1000 mL of 0.2 M HCO_3^- solution at 338 K. The relatively sensitive nature of aurichalcite to acidic (pH<6) conditions precluded the use of the depleting methods mentioned in [53] in order to obtain optimum yields of high phase purity aurichalcite. Saturated sodium bicarbonate was added at a quasi-constant rate in order to maintain a pH≈7.15, the samples were then aged for 30 min at 338 K under constant stirring. Aged samples were vacuum filtered and washed with hot, degassed, demineralised water. Samples were then dried overnight at 373 K.

X-ray diffraction

Powder X-ray diffraction analyses were performed on a Phillips X-ray diffractometer (radius: 173.0 mm). Incident X-ray radiation was produced from a long fine focused C-Tech PW1050 Co. X-ray tube, operating at 40 kV and 32 mA. The incident beam passed through a 1° divergence slit, a 15 mm fixed mask and a 1° fixed anti-scatter slit. The detector was set in scanning mode, with an active length of 2.022 mm. Samples were analysed utilising Bragg–Brentano geometry over a range of 3–75° 2θ with a step size of 0.02° 2θ, with each step measured for 200 s.

Thermal analysis

Thermal decomposition of the aurichalcite samples was carried out in a TA® Instruments incorporated high-resolution thermogravimetric analyzer (series Q500) in a flowing nitrogen atmosphere at a rate of 90 cm^3 min^{-1}. Approximately 20 mg of sample underwent thermal analysis, with a heating rate of 5°C min^{-1}, with high resolution, to 1000°C. With the quasi-isothermal, quasi-isobaric heating program of the instrument the furnace temperature was regulated precisely to provide a uniform rate of decomposition in the main decomposition stage.

The TG instrument was coupled to a Balzers (Pfeiffer) mass spectrometer for EGA. Water vapour, hydroxyl groups, carbon dioxide, mono- and diatomic oxygen were analyzed; diatomic nitrogen was analyzed in order to evaluate the background signal of the spectrometer.

Results and discussion

X-ray diffraction and EDX analysis

The X-ray diffraction patterns for the synthesised aurichalcite together with two reference patterns are shown in Fig. 1. The XRD patterns for Cu/Zn aurichalcite from 0.1/0.9; 0.25/0.75, 0.4/0.6 and 0.5/0.5 are shown. No minor impurities are observed.

Thermal analysis of $Cu_{0.5}$ $Zn_{4.5}(CO_3)_2(OH)_6$

The thermal analysis of the 0.1:0.9 (Cu:Zn) synthetic aurichalcite is shown in Fig. 2a. The ion current curves for the evolved gases of the 0.1:0.9 (Cu:Zn) synthetic aurichalcite are shown in Fig. 2b. A summary of the thermogravimetric analyses are shown in Table 1. This table reports the decomposition temperatures determined as peak maxima in the DTG curves for each of the synthetic aurichalcites studied. Thermal decomposition occurs at 200°C with a mass loss of 2.65%, 224°C with a mass loss of 1.68%. The major mass loss occurs at 255°C with a mass loss of 20.66%.

Table 1 Summary of the TG analyses of the samples according to the Cu/Zn ratio of the synthesized aurichalcites

Decomposition stage	Mineral composition from synthesis									
	50–50 DTG peak maxima		40–60 DTG peak maxima		25–75 DTG peak maxima		20–80 DTG peak maxima		10–90 DTG peak maxima	
1st	220°C	3.77%	225°C	3.77%	235°C	3.95%	228°C	3.55%	200°C	2.65%
2nd	300°C	14.00%	290°C	17.00%	280°C	18.69%	275°C	20.99%	224°C	1.68%
3rd	355°C	1.89%	355°C	2.0%	394°C	2.47%	372°C	2.19%	255°C	20.66%
4th	433°C	7.27%	433°C	7.5%	428°C	2.10%			355°C	1.96%
5th	815°C	3.75%	815°C	4.0%	805°C	1.53%	815°C	1.49%	781°C	0.74%

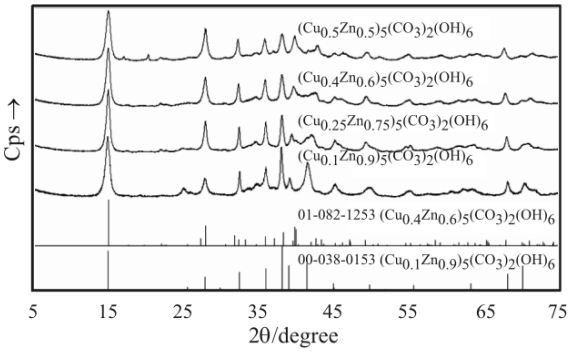

Fig. 1 X-ray diffraction patterns of synthetic aurichalcite as a function of composition

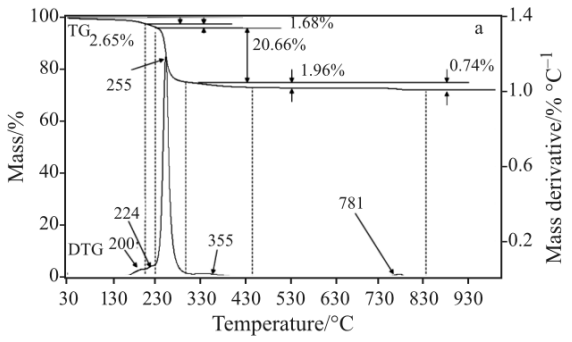

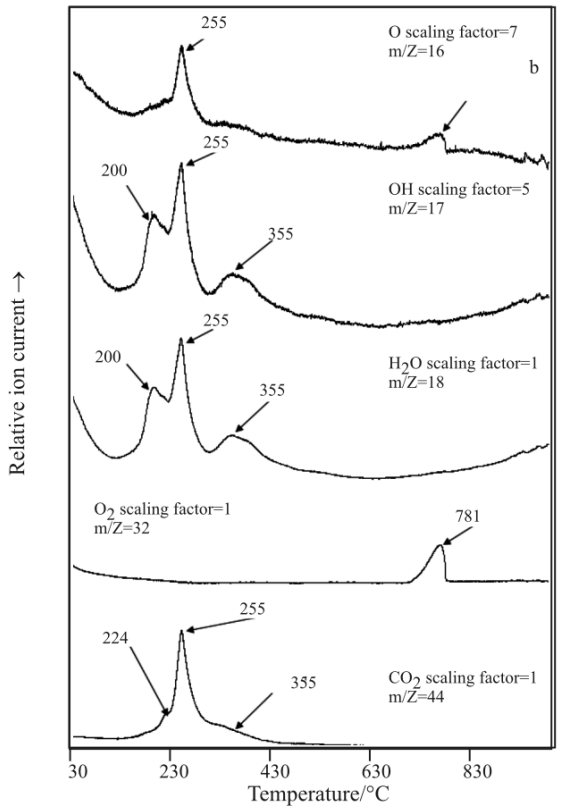

Fig. 2 a – TG and DTG patterns of synthetic aurichalcite of composition $(Cu_{0.1}Zn_{0.9})_5(CO_3)_2(OH)_6$; b – Relative ion current curves of synthetic aurichalcite of composition $(Cu_{0.1}Zn_{0.9})_5(CO_3)_2(OH)_6$

Two other minor thermal decomposition steps are observed at 355 and 781°C.

It is proposed that the following chemical reaction occurs during the thermal decomposition of aurichalcite. At the temperatures 200, 224 and 255°C the following reaction occurs:

$$Cu_{0.5}Zn_{4.5}(CO_3)_2(OH)_6 \rightarrow$$
$$\rightarrow 0.5ZnCO_3+0.5CuCO_3+4ZnO+3H_2O+CO_2$$

The ion current curves (Fig. 2b) give an indication of the thermal decomposition according to the gas evolution. For the ion current curve of m/Z=44 (CO_2) gas evolution occurs at 224, 255 and 355°C. For the m/Z=18 and 17, maxima are observed at 200, 255 and 355°C. This water vapour evolution is assigned to the thermal decomposition of the OH units. Thus it is concluded that fundamentally the CO_2 and OH units are lost simultaneously at 255 and 355°C. The m/Z=16 curve assigned to oxygen evolution shows maximum at 255°C. Thus in the thermal decomposition, the transition of $ZnCO_3$ and $CuCO_3$ to the oxides and then the metal is suggested. The m/Z=16 and 32 show a maxima at 781°C. This gas evolution is attributed to the decomposition of the metal oxides to the metal.

Thermal analysis of $Cu_{1.25}Zn_{3.75}(CO_3)_2(OH)_6$

The thermal analysis of the 0.25:0.75 (Cu:Zn) synthetic aurichalcite is shown in Fig. 3a. The ion current curves for the evolved gases of the 0.25:0.75 (Cu:Zn) synthetic aurichalcite are shown in Fig. 3b. Thermal decomposition of $Cu_{1.25}Zn_{3.75}(CO_3)_2(OH)_6$ is similar to that of $Cu_{0.5}Zn_{4.5}(CO_3)_2(OH)_6$. Five thermal decomposition steps, as determined by the maxima of the DTG peaks, are observed at 235, 280, 394, 428 and 805°C with mass losses of 3.95, 18.69, 2.47, 2.10 and 1.53%. The ion current curve for m/Z=44 indicates CO_2 is lost at 235, 280, 394 and 428°C. The ion current curves for m/Z=17 and 18 show that OH units are lost at the peak maxima of 235 and 280°C. These results suggest that the OH units and carbonate units decompose simultaneously at 235 and 280°C and that the decomposition steps at 394 and 428°C are associated with the decomposition of $ZnCO_3$ and $CuCO_3$. The ion current curve for m/Z=16 shows some oxygen is lost at DTG peak maxima 235, 280, 394 and 428°C. More importantly significant amounts of oxygen are observed in the ion current curve at the peak maximum, of 805°C. It is suggested this results from the decomposition of CuO and ZnO.

Thermal analysis of $Cu_2Zn_3(CO_3)_2(OH)_6$

The thermal decomposition of 2:3 aurichalcite shows two steps at 235 and 280°C with mass losses of 3.95

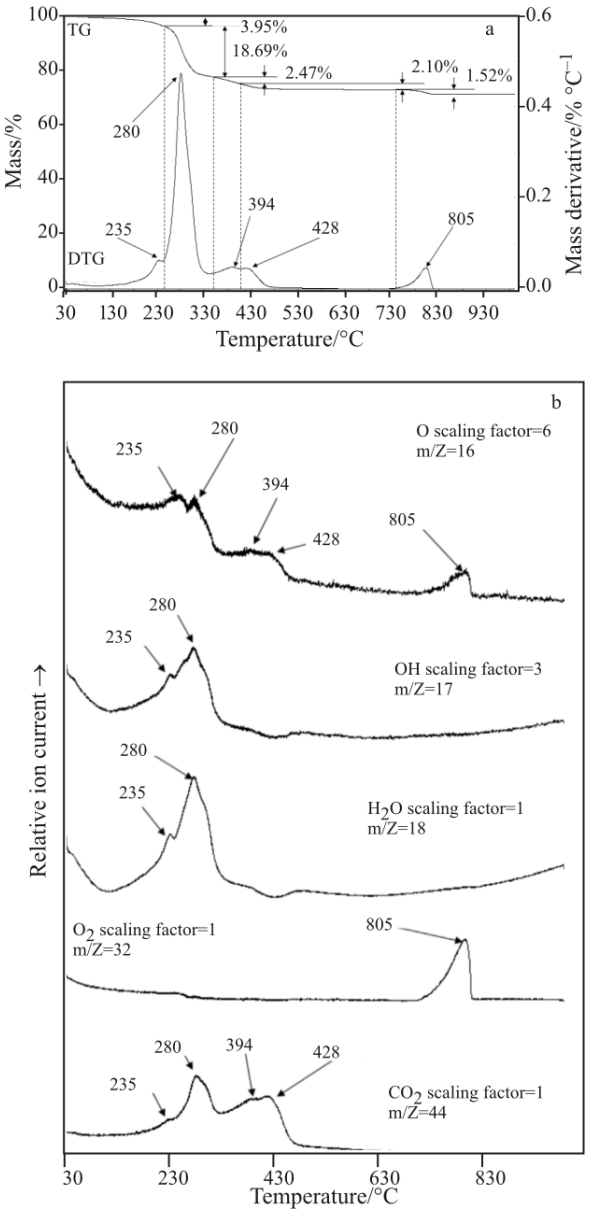

Fig. 3 a – TG and DTG patterns of synthetic aurichalcite of composition $(Cu_{0.25}Zn_{0.75})_5(CO_3)_2(OH)_6$; b – Relative ion current curves of synthetic aurichalcite of composition $(Cu_{0.25}Zn_{0.75})_5(CO_3)_2(OH)_6$

and 18.69%. Two more mass loss steps at 394 and 428°C with mass losses of 2.47 and 2.10% are found. A higher temperature mass loss of 1.53% is observed at 805°C. The maxima in the ion current curves for *m*/*Z*=17 and 18 occurs at 235 and 280°C. This proves that the OH units of aurichalcite are being lost at these temperatures. The theoretical mass loss of OH units is given by 102/546.7=18.66%. The total experimental mass loss at these temperatures is 22.64% i.e. is 3.98% too high. The study of the ion current curves for *m*/*Z*=44 shows that CO_2 is evolved at 235 and 280°C as well as 394 and 428°C. This additional mass loss therefore is attributed to the decomposition of carbonate in aurichalcite. These results support the assumption that CO_2 and H_2O are lost simultaneously.

It is proposed that the following chemical reactions occur during the thermal decomposition of aurichalcite.

- At the DTG peak maxima temperature 235 and 280°C

$$(Zn_2,Cu_3)(CO_3)_2(OH)_6\rightarrow$$
$$\rightarrow ZnCO_3+CuCO_3+4ZnO+4CuO+3H_2O+CO_2$$

- At the temperature 394°C

$$CuCO_3\rightarrow CuO+CO_2$$

The results reported in Fig. 2 shows that some traces of oxygen (*m*/*Z*=16) are lost at 394 and 428°C.

- At the temperature 428°C

$$ZnCO_3\rightarrow ZnO+CO_2$$

- At the temperature 805°C

$$2CuO\rightarrow Cu_2O+1/2O_2$$

$$CuO\rightarrow Cu+1/2O_2$$

The data for *m*/*Z*=32 (Fig. 2) shows that oxygen is liberated at MS peak maxima 805°C. The amount of oxygen expected to be lost theoretically is 2.92%. The amount of oxygen lost at 805°C is 1.53%. The difference may be accounted for by the oxygen which is lost at the ion current maxima of 394 and 428°C.

Thermal analysis of $Cu_{2.5}Zn_{2.5}(CO_3)_2(OH)_6$

The thermal analysis of the 0.5:0.5 (Cu:Zn) synthetic aurichalcite is shown in Fig. 4a. The ion current curves for the evolved gases of the 0.5:0.5 (Cu:Zn) synthetic aurichalcite are shown in Fig. 4b. The principal mass loss occurs at DTG peak maxima of 300°C with a 14% mass loss. A small mass loss of 1.89% occurs at 355°C. A large mass loss of 7.2% is found at DTG peak maxima of 433°C. A higher temperature mass loss of 3.75% occurs at 815°C. The ion current curves (*m*/*Z*=17 and 18) for this thermal decomposition show that H_2O is the evolved gas at 300 and 355°C. The ion current curves for *m*/*Z*=44 show that CO_2 is evolved at 229, 300, 355 and 433°C. The ion current curve for *m*/*Z*=32 shows that O_2 is evolved at 815°C. The results support the assumption for the 2:3 aurichalcite that OH units and $(CO_3)^{2-}$ units decompose simultaneously.

The effect of composition on the thermal decomposition of synthetic aurichalcite

Figure 5 displays the effect of change in the chemical composition on the DTG curves of the synthetic aurichalcite. This figure clearly shows that the effect

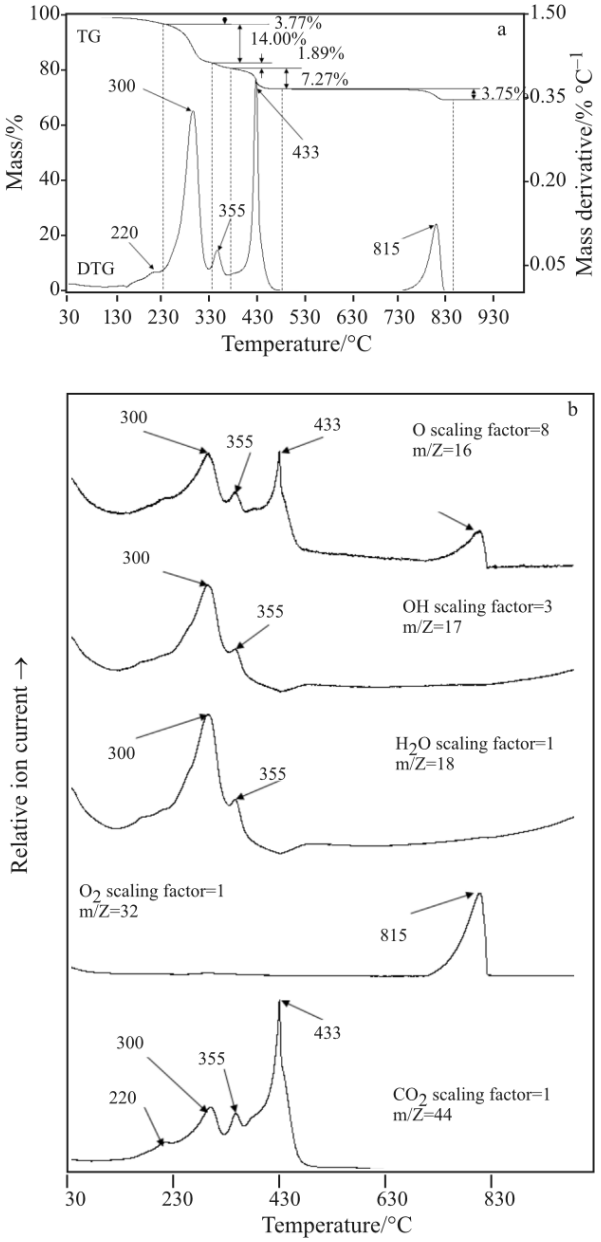

Fig. 4 a – TG and DTG patterns of synthetic aurichalcite of composition $(Cu_{0.5}Zn_{0.5})_5(CO_3)_2(OH)_6$; b – Relative ion current curves of synthetic aurichalcite of composition $(Cu_{0.5}Zn_{0.5})_5(CO_3)_2(OH)_6$

of increasing the Cu content of the hydrotalcite results in the increase in temperature of the principle thermal decomposition step. For 10/90 Cu/Zn the maximum in the DTG curve occurs at DTG peak maxima 255°C; for 20/80 the peak is at DTG peak maxima 275°C; for 25/75 the peak is at DTG peak maxima 280°C. As the Cu content is increased the peak shifts to 300°C. This implies the synthesised aurichalcites with higher Cu content are more stable.

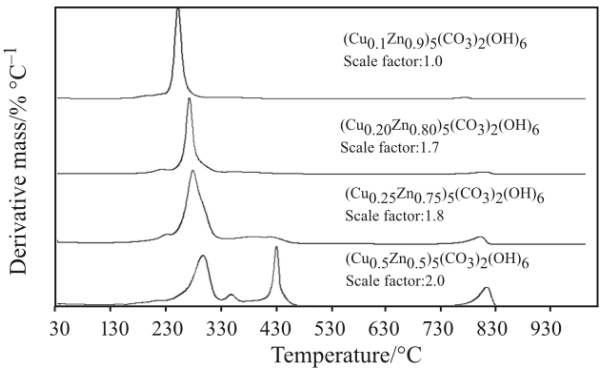

Fig. 5 Variation in the peak maximum decomposition temperature with % composition

Conclusions

Synthetic aurichalcite was prepared with variation of the Cu/Zn ratio from 0.1/0.9 to 0.5/0.5. Thermal decomposition of aurichalcite provides a method for preparing mixed oxide catalysts [54]. This research reports methodology for the synthesis of mixed CuO–ZnO mixed metal oxides based upon the thermal decomposition of aurichalcite. Because the thermal decomposition of aurichalcite results in the evolution of water and CO_2, it means that the mixed metal oxides can be formed with high purity and are mixed at the molecular level rather than the particulate level. The effect of increasing the Cu/Zn ratio results in an increase in the temperature of decomposition of the aurichalcite. This variation is shown in Fig. 5. The DTG peak temperature of the synthetic aurichalcite increases with % CuO. Thus certain mixed oxides may be better for application as photocatalysts because of higher thermal stability.

Acknowledgements

The financial and infrastructure support of the Queensland University of Technology Inorganic Materials Research Program of the School of Physical and Chemical Sciences is gratefully acknowledged. The Australian Research Council (ARC) is thanked for funding the thermal analysis facility.

References

1 R. S. Braithwaite and G. Ryback, Mineral. Mag., 33 (1963) 441.
2 R. G. Herman, C. E. Bogdan, P. L. Kumler and D. M. Nuszkowski, Mater. Chem. Phys., 35 (1993) 233.
3 J. L. Jambor, Can. Mineral., 8 (1964) 92.
4 B. J. Reddy and R. L. Frost, J. Near Infrared Spectrosc., 15 (2007) 115.
5 R. L. Frost, J. Raman Spectrosc., 37 (2006) 910.

6 R. L. Frost, D. L. Wain, W. N. Martens and B. J. Reddy, Polyhedron, 26 (2007) 275.
7 R. L. Frost, B. J. Reddy, D. L. Wain and W. N. Martens, Spectrochim. Acta, Part A, 66 (2007) 1075.
8 R. L. Frost, D. L. Wain, W. N. Martens and B. J. Reddy, Spectrochim. Acta, Part A, 66 (2007) 1068.
9 P. A. Williams, Oxide Zone Geochemistry, Ellis Horwood Ltd., Chichester, West Sussex, England 1990.
10 G. Sengupta, R. K. Sharma, V. B. Sharma, K. K. Mishra, M. L. Kundu, R. M. Sanyal and S. Dutta, J. Solid State Chem., 115 (1995) 204.
11 J. W. Anthony, R. A. Bideaux, K. W. Bladh and M. C. Nichols, Handbook of Mineralogy, Mineral Data Publishing, Tiscon, Arizona, USA 2003.
12 J. L. Jambor and I. D. MacGregor, Paper - Geological Survey of Canada 74-1, Pt. B (1974) 172.
13 M. M. Harding, B. M. Kariuki, R. Cernik and G. Cressey, Acta Crystallogr., Section B: Struct. Sci., B50 (1994) 673.
14 J. M. Bouzaid, R. L. Frost, A. W. Musumeci and W. N. Martens, J. Therm. Anal. Cal., 86 (2006) 745.
15 R. L. Frost, J. M. Bouzaid, A. W. Musumeci, J. T. Kloprogge and W. N. Martens, J. Therm. Anal. Cal., 86 (2006) 437.
16 R. L. Frost and Z. Ding, Thermochim. Acta, 397 (2003) 119.
17 R. L. Frost and Z. Ding, Thermochim. Acta, 405 (2003) 207.
18 R. L. Frost, Z. Ding and H. D. Ruan, J. Therm. Anal. Cal., 71 (2003) 783.
19 R. L. Frost, K. L. Erickson, M. L. Weier, A. R. McKinnon, P. A. Williams and P. Leveret, Thermochim. Acta, 427 (2005) 167.
20 R. L. Frost, J. Kristóf, W. N. Martens, M. L. Weier and E. Horváth, J. Therm. Anal. Cal., 83 (2006) 675.
21 R. L. Frost, W. Martens and M. O. Adebajo, J. Therm. Anal. Cal., 81 (2005) 351.
22 R. L. Frost, D. L. Wain, R.-A. Wills, A. Musemeci and W. Martens, Thermochim. Acta, 443 (2006) 56.
23 R. L. Frost and M. L. Weier, Thermochim. Acta, 409 (2004) 79-85.
24 R. L. Frost and M. L. Weier, Thermochim. Acta, 406 (2003) 221.
25 R. L. Frost, M. L. Weier and W. Martens, J. Therm. Anal. Cal., 82 (2005) 373.
26 R. L. Frost, R.-A. Wills, J. T. Kloprogge and W. Martens, J. Therm. Anal. Cal., 84 (2006) 489.
27 R. L. Frost, R.-A. Wills, J. T. Kloprogge and W. N. Martens, J. Therm. Anal. Cal., 83 (2006) 213.
28 R. L. Frost and K. L. Erickson, J. Therm. Anal. Cal., 76 (2004) 217.
29 R. L. Frost, K. Erickson and M. Weier, J. Therm. Anal. Cal., 77 (2004) 851.
30 R. L. Frost, M. L. Weier and K. L. Erickson, J. Therm. Anal. Cal., 76 (2004) 1025.
31 R. L. Frost and M. L. Weier, J. Therm. Anal. Cal., 75 (2004) 277.
32 R. L. Frost, W. Martens, Z. Ding and J. T. Kloprogge, J. Therm. Anal. Cal., 71 (2003) 429.
33 Y. Zhao, R. L. Frost, W. N. Martens and H. Y. Zhu, J. Therm. Anal. Cal., 90 (2007) 755.
34 R. L. Frost, A. W. Musumeci, M. O. Adebajo and W. Martens, J. Therm. Anal. Cal., 89 (2007) 95.
35 A. W. Musumeci, G. G. Silva, W. N. Martens, E. R. Waclawik and R. L. Frost, J. Therm. Anal. Cal., 88 (2007) 885.
36 R. L. Frost, A. W. Musumeci, J. T. Kloprogge, M. L. Weier, M. O. Adebajo and W. Martens, J. Therm. Anal. Cal., 86 (2006) 205.
37 R. L. Frost, W. N. Martens and K. L. Erickson, J. Therm. Anal. Cal., 82 (2005) 603.
38 R. L. Frost, M. L. Weier and W. Martens, J. Therm. Anal. Cal., 82 (2005) 115.
39 Y. Xi, W. Martens, H. He and R.L. Frost, J. Therm. Anal. Cal., 81 (2005) 91.
40 Y.-H. Lin, M. O. Adebajo, R. L. Frost and J. T. Kloprogge, J. Therm. Anal. Cal., 81 (2005) 83.
41 R. L. Frost, J. Kristóf, M. L. Weier, W. N. Martens and E. Horváth, J. Therm. Anal. Cal., 79 (2005) 721.
42 R. L. Frost and K. L. Erickson, J. Therm. Anal. Cal., 78 (2004) 367.
43 C. W. Beck, Am. Mineral., 35 (1950) 985.
44 V. P. Ivanova, Zapiski Vserossiiskogo Mineralogicheskogo Obshchestva, 90 (1961) 50.
45 J. Bandara, I. Guasaquillo, P. Bowen, L. Soare, W. F. Jardim and J. Kiwi, Langmuir, 21 (2005) 8554.
46 A. Chatzitakis, C. Berberidou, I. Paspaltsis, G. Kyriakou, T. Sklaviadis and I. Poulios, Water. Res., 42 (2008) 386.
47 F.-Z. Deng, A.-X. Zhu and R. Yang, Guangpuxue Yu Guangpu Fenxi, 26 (2006) 299.
48 A. Dodd, A. McKinley, M. Saunders and T. Tsuzuki, Nanotechnology, 17 (2006) 692.
49 V. K. Ivanov, A. S. Shaporev, F. Y. Sharikov and A. Y. Baranchikov, Superlattices Microstr., 42 (2007) 421.
50 M. A. Messikh and T. Sehili, J. Société Algérienne de Chimie, 9 (1999) 165.
51 H. Wang, C. Xie, W. Zhang, S. Cai, Z. Yang and Y. Gui, J. Hazardous Mater., 141 (2007) 645.
52 S.-I. Fujita, Y. Kanamori, A. M. Satriyo and N. Takezawa, Catal. Today, 45 (1998) 241.
53 G. J. Millar, I. H. Holm, P. J. R. Uwins and J. Drennan, J. Chem. Soc., Faraday Trans., 94 (1998) 593.
54 G.-C. Shen, S.-I. Fujita, S. Matsumoto and N. Takezawa, J. Mol. Catal. A: Chemical, 124 (1997) 123.

Received: July 11, 2007
Accepted: April 8, 2008
OnlineFirst: August 15, 2008

DOI: 10.1007/s10973-007-8634-2